Pleistocene Diversification of the *Odontophotopsis unicornis* Species-Group (Hymenoptera: Mutillidae)

JOSEPH S. WILSON[1] AND JAMES P. PITTS

Department of Biology, Utah State University, 5305 Old Main Hill, Logan, UT 84322-5305

Ann. Entomol. Soc. Am. 103(4): 555–565 (2010); DOI: 10.1603/AN09177

ABSTRACT Many recent studies have suggested that a majority of the species-level diversification in the arid-adapted North American biota was driven by mountain-building events that took place in the late Neogene (15–2 Ma). This assertion was tested with a phylogeographic analysis of the *Odontophotopsis unicornis* species-group by using the rDNA internal transcribed spacer regions internal transcribed spacer (ITS)1 and ITS2 and a Bayesian methodology. The validity of the two species in this species-group [*Odontophotopsis unicornis* Schuster and *Odontophotopsis erebus* (Melander)] was tested both morphologically and molecularly. The female of *O. unicornis* was previously unknown and was associated with the male using molecular data. Here, *O. unicornis* is described and compared with that of its sister species *O. erebus*. Divergence dates for the *O. unicornis* species-group were estimated using the programs r8s and BEAST and calibrated with fossils from Dominican amber. These analyses resulted in a well supported phylogenetic tree that reinforces the notion that *O. unicornis* and *O. erebus* are distinct species. Little or no phylogenetic structuring was found among populations of either species. The species in this group seem to have evolved in the middle Pleistocene (≈1 Ma). The lack of phylogeographic structuring in each of the species of the *O. unicornis* species-group is probably due to the recent origin of these species. This analysis represents one of the few instances of Pleistocene age species-level divergences in desert-adapted taxa.

KEY WORDS biogeography, phylogeography, desert, Sphaeropthalminae, velvet ants

Phylogeographic analyses use the genetic population structure within widespread species and among closely related species to understand their geographic distributions and gain insight into the geobiotic history of a region (Avise 2000). Many recent studies have suggested that a majority of the species-level diversification in the arid-adapted North American biota was driven by Neogene vicariant events (i.e., mountain-building events) rather than by Pleistocene climatic oscillations (Riddle 1995, Orange et al. 1999, Douglas et al. 2006). It is clear, however, that the Pleistocene climate change had a large effect on the distribution and population-level divergence within species, but the importance of these climatic oscillations to the macroevolutionary dynamics is debatable (Klicka and Zink 1997).

Velvet ants (Hymenoptera: Mutillidae) are an often unnoticed yet common element of North America's desert environments. All velvet ants are solitary parasitic wasps that parasitize other aculeate Hymenoptera, including bees (Apoidea) (Krombein 1979, Nonveiller 1990, Brothers 1995). Although the colorful, diurnal species are most frequently encountered, a rich and abundant fauna of nocturnal velvet ants also exists. With >205 known nocturnal species in nine genera found throughout western North America, members of this family are ideal subjects for revealing phylogeographic patterns in the deserts and arid regions (Pitts et al. 2010).

The *Odontophotopsis unicornis* species-group currently contains only the species *Odontophotopsis erebus* (Melander) and *Odontophotopsis unicornis* Schuster (Pitts 2007). The species-group is easy to recognize and is distinctive among the North American nocturnal mutillid fauna due, in part, to unique clypeal and mandibular morphology (Pitts 2007). The distinction between the species in this group, which is based on differences in the length of the clypeal tubercle and on very slight differences in the genitalia, can be occasionally difficult to discern. Because of the morphological similarities within the species-group, Pitts (2007) suggested that future molecular studies may show that these two species represent one highly variable species.

Extreme sexual dimorphism occurs in mutillids, with the result that many species and even genera are known only from a single sex (Brothers 1995). Sex associations for the nocturnal velvet ants are further compounded by the great morphological similarity of the species, and because although males are easily collected with light traps, females are rarely caught. Molecular techniques are now available to make sex

[1] Corresponding author, e-mail: joseph.wilson@usu.edu.

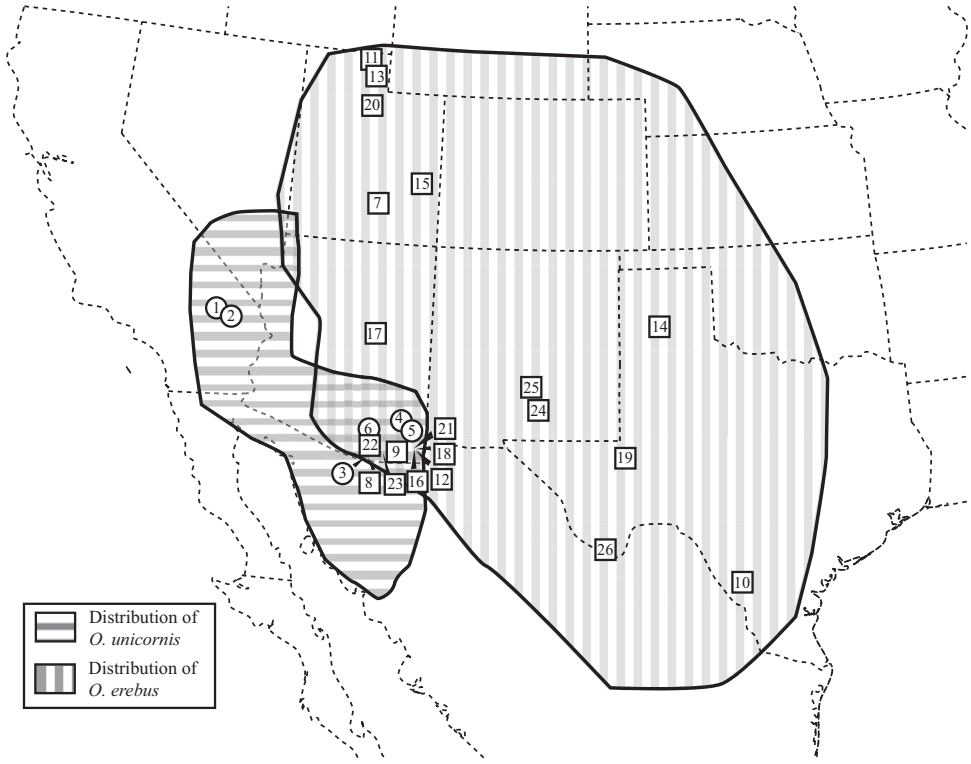

Fig. 1. Map of Western North America showing the distributions of *O. erebus* and *O. unicornis* based on Pitts (2007). Collection locations for the specimens used in the phylogeographic analysis also are shown with circles representing *O. unicornis* and squares representing *O. erebus*. Numbers inside each symbol correspond to Figs. 1 and 4 and Table 1.

associations using species-specific genetic loci (Pilgrim and Pitts 2006, Pitts et al. 2007, Pilgrim et al. 2008). Historically, the species in the *O. unicornis* species-group were known only from males. The female of *O. erebus* was only recently described (Pitts et al. 2007), whereas the female of *O. unicornis* remains unknown. Discovering the female of *O. unicornis* can add to our understanding of the species-group by making available morphological characters of the female, which may better define the species boundaries within the group.

The biogeographical pattern of the *O. unicornis* species-group is also interesting. One member, *O. erebus*, is wide ranging from western Kansas, Nebraska, Oklahoma, and Texas west to Arizona, Nevada, New Mexico, and Utah, and south into northern Mexico. This species, however, is absent from the Mojave and western Sonoran deserts. The other member, *O. unicornis*, is found in the Sonoran and Mojave deserts of Arizona, Nevada, and California into northern Mexico. The ranges of these two species overlap broadly in the eastern Sonoran Desert over most of southern Arizona. This overlap leads one to further question the distinctness of these two species.

The purposes of this study are to 1) determine the validity of the species in the *O. unicornis* species-group by using both molecular and morphological data; 2) uncover any phylogeographic patterns within this species-group and associate the genetic divergences with historical geological or climatological events, by using molecular dating techniques calibrated with fossil data and determine whether the there is good evidence for discrete species; and 3) describe and associate the female of *O. unicornis*.

Materials and Methods

Trapping Methods. During summers 2005–2008, field studies were conducted throughout the southwestern United States to collect fresh specimens of both sexes of nocturnal velvet ants. Collections were made of male and female nocturnal mutillids at 60 field sites across the southwestern United States. Specimens were collected using blacklight traps, fluorescent lantern traps, and by hand. Those collected with light traps were captured in soapy water and were transferred into 95% ethanol, whereas all hand-collected specimens were placed directly into 95% ethanol. All specimens were identified to the species level except for some female specimens that were sorted to morphospecies because they had not yet been associated with males. Samples were collected from various sites across the range of each species in the *O. unicornis* species-group (Fig. 1). In total, 20 *O. erebus* specimens (19 males and one female) were sampled, as well as four male *O. unicornis* specimens. Also, two unknown female specimens that were morphologically similar to the female of *O. erebus* were included.

All specimens were examined for both morphological and molecular characters.

Molecular Methods. Molecular techniques including, DNA extraction, polymerase chain reaction (PCR), and sequencing were preformed following the protocol described by Pilgrim and Pitts (2006). The following primers were used to amplify the internal transcribed spacer (ITS)1 and ITS2 regions of the nuclear genome. The primers 5′-GATTACGTCCCTGCCCTTTG-3′ (forward-18S) and 5′-CGATGATCAAGTGTCCTGCA-3′ (reverse-5.8S) (both from Pilgrim et al., 2002) were used for the ITS1 locus and 5′-GGCTCGTGGAATCGATGAAGAACG-3′ (forward 5.8S) (modified from Weekers et al., 2001) and 5′-GCTTATTAATATGCTTAAATTCAGCGG-3′ (Weekers et al. 2001) were used for ITS2. PCR took place in a 20-μl volume with conditions of 3 mM $MgCl_2$, 200 pM dNTPs, 2 U of *Taq* polymerase, 1 mM each primer, and standard PCR buffer concentration. For each PCR, ≈20 ng of template DNA was added to the reaction. The PCR program included an initial step of 94°C for 150 s, followed by 35 cycles of 94°C for 30 s, 52°C (ITS1) or 56°C (ITS2) for 60 s, and 72°C for 60 s, with a final step of 72°C for 10 min. Amplified products were visualized on agarose gels stained with ethidium bromide. Successful PCR products were cleaned using isopropanol purification.

ITS1 and ITS2 were sequenced for representatives of each available species and sex, sequences were aligned, and females were associated with males based on identical or nearly identical DNA sequences for those loci (i.e., very small genetic distances). The methods proposed by Pilgrim and Pitts (2006) were followed for performing sex associations. ITS1 and ITS2 were sequenced for at least one female of each morphospecies and several male specimens of each described species. PCR was used to amplify the ITS1 and ITS2 regions of the nuclear genome. Gel electrophoresis of each gene yielded a single band for each individual wasp and the resulting DNA was sequenced cleanly, suggesting no gene heterogeneity as seen in some other organisms (Harris and Crandall 2000, Parkin and Butlin 2004, Bower et al. 2008). PCR products were sequenced in both directions and sequence contigs assembled using Sequencher 4.0 (Gene Code Corp., Ann Arbor, MI). DNA sequences were aligned using Clustal W (Thompson et al. 1994) and intraspecfic and interspecific genetic distances were calculated from these alignments. Genetic distances between species were calculated as pairwise percentages by determining the number of differences (point mutations and insertions or deletions) divided by the number of base pairs of the longer of the two sequences. ITS1 and ITS2 sequences were deposited in GenBank (accessions HM030444–HM030491; Table 1).

Phylogenetic and Haplotype Network Methods. The two genetic loci were subjected to Bayesian analysis using MrBayes version 3.1.2 (Ronquist and Huelsenbeck 2003). Sequences were analyzed as a combined data set, with each gene partitioned separately with all parameters unlinked across loci. Appropriate models of nucleotide substitution were determined in MrModeltest version 2.3 (Nylander 2004). Bayesian analyses included four independent runs with three heated chains and one cold chain in each run. The Markov chain Monte Carlo (MCMC) chains were set for 3,000,000 generations and sampled every 100 generations; chains were run until the average SD of the split frequencies dropped below 0.01. The burn-in period for each analysis was removed after graphical determination of stationarity. Several outgroups were included in the analysis. *Odontophotopsis rubiventris* (Schuster) and *Odontophotopsis armata* Schuster are closely related to the *O. unicornis* species-group (Pitts et al. 2010) and were included. *Odontophotopsis delodonta* Viereck was used as a more distant outgroup. In addition to the full phylogenetic analysis, a Bayesian analysis was implemented on a subset of the full data set to streamline the molecular dating process. Included in this analysis were two *O. erebus* populations, two *O. unicornis* populations, the same outgroups as were used in the full phylogenetic analysis, and multiple *Dasymutilla* species, including *Dasymutilla snoworum* (Cockerell), *Dasymutilla occidentalis* (L.), *Dasymutilla gloriosa* (Saussure), and a *Traumatomutilla* species. These additional outgroups were added to include a fossil for calibration in the molecular dating analysis.

A parsimony-based haplotype network was constructed using the combined ITS1 and ITS2 sequences for all *Dilophotopsis* specimens by using TCS version 1.21 (Clement et al. 2000). The program estimated the 95% reconnection limit between haplotypes with gaps treated as missing data.

Molecular Dating Methods. Divergence date estimates were calculated for major nodes on the tree using two methods: a penalized likelihood approach to rate smoothing using the program r8s 1.71 (Sanderson 2003), and a Bayesian MCMC averaging approach to rate smoothing using the program BEAST version 1.4.8 (Drummond and Rambaut 2007). Because there is a disparity of fossils that can be used as calibration points in Mutillidae, two distinct dating methods were used as a way to corroborate the divergence date. Although no fossils are available for *Odontophotopsis* or any of the nocturnal velvet ants, two fossils from Dominican amber, *Dasymutilla dominica* Manley & Poinar and *Dasymutilla albifasciatus* Manley & Poinar (Manley and Poinar 1991, 1999, 2003) were used to calibrate the estimated divergence dates. Based on the morphology of these fossils, they seem to be most closely related to the basal members of the genus *Dasymutilla* (Pitts et al. 2010).

r8s Analysis. The program r8s uses a tree description with branch lengths to estimate divergence dates. The consensus tree that resulted from the paired down Bayesian analysis was used in the r8s analysis. The most recent common ancestor (MRCA) of the *Dasymutilla* plus *Traumatomutilla* clade was constrained to be at least 20 Ma (minage = 20) based on the placement of the fossils and the reported age of Dominican amber (Iturralde-Vinent and MacPhee 1996). The root was fixed at 65 million yr based on the estimated maximum age of Mutillidae (Grimaldi and Engel 2005), and the penalized likelihood method

Table 1. Descriptive information for all taxa used in the phylogenetic portion of this study

Species	Species ID no. (see Figs. 1, 2, 4)	Voucher ID	Sex	Collection location	ITS1 accession no.	ITS2 accession no.
D. snoworum	NA	JP443	F	TX: Hidalgo Co., Bensten-Rio Grande Valley State Park	GU814282	GU814407
D. occidentalis	NA	Moccf	F	SC: Florence Co., Florence, Pee Dee Research and Education Center	GU814283	GU814408
D. gloriosa	NA	JP242	F	AZ: Cochise Co., 2 mi S Willcox	DQ408505	DQ408505
Traumatomutilla sp.	NA	JP621	F	Bolivia: Santa Cruz, 5 km SSE Burna Vista	GU814284	GU814409
O. delodonta	NA	JP337	M	AZ: Santa Cruz Co., 5 km W Peña Blanca Lake	HM030489	HM030465
O. rubiventris	NA	JP442	M	TX: Hidalgo Co., Bensten Rio Grand State Park	GU814301	GU814428
O. armata	NA	JP466	M	AZ: Maricopa Co., 23 mi NW Gila Bend	GU814316	GU814442
O. unicornis	1	JP635	M	CA: San Bernardino Co., Afton Canyon	HM030475	HM030451
O. unicornis	2	JP634	M	CA: San Bernardino Co., Afton Canyon	HM030474	HM030450
O. unicornis	3	JP547	M	AZ: Santa Cruz Co., Sycamore Canyon, 3.5 mi SE Ruby	HM030473	HM030449
O. unicornis	4	JP295	F	AZ: Cochise Co., 2 mi S Willcox	HM030491	HM030467
O. unicornis	5	JP348	F	AZ: Cochise Co., 2 mi S Willcox	HM030490	HM030466
O. unicornis	6	JP134	M	AZ: Pima Co., Santa Rita Experimental Range, Florida Wash	GU814331	GU814457
O. erebus	7	JP550	M	UT: Garfield Co., Calf Creek, 10 km S Boulder	HM030472	HM030448
O. erebus	8	JP544	M	AZ: Santa Cruz Co., Sycamore Canyon, 3.5 mi SE Ruby	HM030481	HM030457
O. erebus	9	JP537	M	AZ: Cochise Co., Carr Canyon	HM030487	HM030463
O. erebus	10	JP530	M	TX: La Salle Co., Chaparral Wildlife Management Area	HM030476	HM030452
O. erebus	11	JP230	F	UT: Cache Co., Hyrum Reservoir	DQ415675	DQ415675
O. erebus	12	JP546	M	AZ: Cochise Co., Chiricahua Mtns., Cave Creek Rd.	HM030471	HM030447
O. erebus	13	JP229	M	UT: Cache Co., Hyrum Reservoir	DQ415674	DQ415674
O. erebus	14	JP531	M	TX: Randall Co., Palo Duro Canyon State Park	HM030477	HM030453
O. erebus	15	JP535	M	UT: Grand Co., Moab	HM030478	HM030454
O. erebus	16	JP538	M	AZ: Cochise Co., Chiricahua Mtns., Paradise Rd., 3 mi W Portal	HM030478	HM030455
O. erebus	17	JP540	M	AZ: Yavapi Co., nr Montezuma Castle State Park	HM030480	HM030456
O. erebus	18	JP548	M	AZ: Cochise Co., Southwestern Research Station	HM030482	HM030458
O. erebus	19	JP549	M	TX: Ward Co., Monahans Sand Hills State Park	HM030483	HM030459
O. erebus	20	JP545	M	UT: Davis Co., Farmington Canyon	HM030484	HM030460
O. erebus	21	JP541	M	AZ: Cochise Co., Chiricahua Mtns., Paradise Rd., 2.5 mi W Portal	HM030485	HM030461
O. erebus	22	JP539	M	AZ: Santa Rita Co., Madera Canyon	HM030486	HM030462
O. erebus	23	JP534	M	AZ: Santa Cruz Co., 2 mi SW Patagonia	HM030488	HM030464
O. erebus	24	JP543	M	NM: Otero Co., 1.8 mi W Oliver Lee Memorial State Park	HM030470	HM030446
O. erebus	25	JP536	M	NM: Otero Co., 5 mi E La Luz	HM030469	HM030445
O. erebus	26	JP529	M	TX: Brewster Co., Big Bend Ranch State Park	HM030468	HM030444

with the truncated Newton algorithm was implemented to estimate rates and divergence dates.

BEAST Analysis. The program BEAST uses the aligned sequence data to generate a tree and estimate divergence dates. The program BEAUtiv1.4.8 (Drummond and Rambaut 2007) was used to generate the file used in BEAST with the alignment of the paired down data set. The MRCA of the *Dasymutilla* plus *Traumatomutilla* clade was constrained to be $\approx$ 20 Ma by giving this node a normally distributed prior with a mean age of 20 million yr and an SD of 1.0. The root node was limited to a mean age of 65 million yr with a SD of 15 million yr based on the estimated age of the family (Grimaldi and Engel 2005). A Yule process speciation prior for branching rates was implemented and the general time-reversible model with invariant sites and gamma-distributed rate variation across sites (GTR+I+Γ) was applied with base frequencies estimated during the analysis. An uncorrelated log-normal model was applied to estimate the relaxed molecular clock because this model places higher prior-density closer to the observed fossil age (Leaché and Mulcahy 2007). The analysis was run using the default MCMC parameters.

Taxonomic Methods and Terminology. The following abbreviations are for institutions or collections housing the material discussed in the current study: Department of Entomology, Academy of Natural Sciences, Philadelphia, PA (ANSP); Department of Entomology and Entomological Museum, Department of Biology, Utah State University, Logan, UT (EMUS); and National Museum of Natural History, Smithsonian, Washington, DC (NMNH).

Based on Ferguson (1967), we adopt the following notation for punctures in the order of decreasing coarseness: reticulate, coarse, moderate, small, fine and micropunctate. Micropunctate refers to punctures that are extremely shallow and do not have vertical walls or sharp margins. Small refers to punctures that do have slight vertical walls and are separated by at least 5$\times$ their diameter. We use the term "Brachyplumose setae" for setae with barbs that are less than, or equal to, the diameter of the shaft at the attachment of the barb. The term "plumose setae" is used for setae that have longer barbs. The term "tibial spurs" is used instead of "calcaria." The abbreviations T2, T3, etc., denote the second, third, etc., metasomal tergites, respectively. Similarly, S2, S3, etc., sig-

nify the second, third, etc., metasomal sternites, respectively.

Results

Molecular Results. Genetic distances were low among populations of a single species. For *O. unicornis*, all ITS1 sequences were identical and for ITS2 the distances were from 0.0 to 0.2%. For *O. erebus*, distances were similarly low, with 0.0–0.4% for ITS1 and 0.0–0.1% for ITS2. Interspecific distances, however, were higher, with a distance of 1.2% for ITS1 and 2.0% for ITS2. Genetic distances of the unknown females, which resembled the female of *O. erebus*, to the males of *O. unicornis* were low (0% for ITS1 and 0.2% for ITS2).

Phylogenetic, Haplotype Network, and Dating Results. The best-fit nucleotide substitution model selected for each gene was the general time-reversible model (GTR) (Lanave et al. 1984). Bayesian analysis of the combined ITS1 and ITS2 data set resulted in a well supported tree with posterior probabilities of 1.0 for most nodes (Fig. 2). The topology showed two distinct clades in the *O. unicornis* species-group, one clade made up of *O. unicornis* populations and the other clade consisting of *O. erebus* populations (Fig. 2). There was no resolution within the *O. unicornis* clade but one subclade was present in the *O. erebus* clade, which was made up of populations from the Chihuahuan Desert. The analysis on the paired down data set to be used in the molecular dating analysis resulted in a tree depicting the same relationships among ingroup taxa as the consensus tree from full analysis (Fig. 3).

Both molecular dating analyses resulted in similar date estimates for the divergence between *O. unicornis* and *O. erebus.* The analysis using the program r8s suggested that these species diverged at ≈1.2 Ma, and the analysis using the program BEAST suggested a divergence date of 0.77 Ma (95% credibility dates from ≈9.5 to 0.5 Ma). The haplotype network analysis resulted in two haplotypes, one halotype representing *O. unicornis* populations and one halotype representing *O. erebus* populations (Fig. 4). Similar to the phylogeny, there is little genetic structuring in the haplotype networks.

Morphological Results. Careful examination of numerous specimens of both species in the *O. unicornis* species-group revealed consistent morphological differences between the males of *O. erebus* and *O. unicornis.* Study of the clypeal tubercle has revealed that this structure on *O. erebus* is an extension of the base of the clypeus, whereas the tubercle of *O. unicornis* is an extension of both the clypeus and the frons (Figs. 5–7). The genitalia are not informative for separating these two species (see Figs. 9–12).

Based on the above-mentioned molecular and morphological data, we are describing the female of *O. unicornis.* Also, we provide diagnoses of the *O. unicornis* species-group and for each of the species in this group.

Odontophotopsis unicornis Species-Group

Diagnosis of Male. This species-group is easily characterized by the unique mandibles (see Fig. 8), which are bidentate apically with a weak ventral excision, a weak-to-moderate ventrobasal angulation or tooth, and dorsal and ventral margins that are sharply and strongly carinate appearing somewhat lamellate (Figs. 5–8). This species-group also has a pair of small, triangulate, mesosternal spines; is nocturnal, having testaceous to stramineous integumental coloration and large ocelli; and has dense fringes of dense plumose setae located on the apices of the metasomal segments. Additional characters can be found in Pitts (2007).

Diagnosis of Female. The female of this species-group can be diagnosed by the following unique combination of characters: the first metasomal segment is petiolate with the second; the sides of the propodeum are punctate; the pygidium is laterally defined by carinae with weak longitudinally striate sculpturing; the mandibles have a distinct basal angulate tooth on ventral margin; and the coloration and setal pattern, specifically the presence of the various colors of decumbent setae and the density of plumose setae composing the metasomal fringes, is characteristic.

Remarks. The females of *O. erebus* and *O. unicornis* are similar to *O. succinea* Viereck in that they both have distinctly margined pygidium both laterally and apically. They differ from both *O. succinea* and *Odontophotopsis melicausa* (Blake) by the lack of transverse sinuate carinae on the mesosomal dorsum and by the lack of a large basal tooth on the ventral margin of the mandible. These two females are also quite similar to *Sphaeropthalma diomeda* (Fox) and *Sphaeropthalma halcyone* (Fox), and it is possible that the latter two species actually belong in *Odontophotopsis.* Although these latter two species have well developed basal teeth on the ventral margin of the mandible, they may be confused with *O. erebus* due to similarities in coloration, but the ventral mandibular tooth in *O. erebus* is not as well developed. Pitts et al. (2007) suggested informally that *S. diomeda* and *O. erebus* may be synonymous given that they differ only in coloration of the metasomal setal fringes. After studying several more female specimens of *O. erebus*, this is no longer believed to be the case given differences in mandibular morphology, as well as head shape and pygidial sculpturing.

Odontophotopsis erebus (Melander)

Mutilla erebus Melander, 1903. Am. Entomol. Soc. Trans. 29: 312. Male. Holotype: New Mexico, Mesilla, T.D.A. Cockerell (NMNH).

Odontophotopsis avellanus Viereck, 1904. Am. Entomol. Soc. Trans. 30: 88. Male. Holotype: Texas (ANSP).

Diagnosis of Male. This species can be distinguished from *O. unicornis* by the clypeus being concave and having a tuberculate process at median proximal margin that is not longer than wide (Fig. 7). Also, the dorsal carina of the mandible is present on the distal

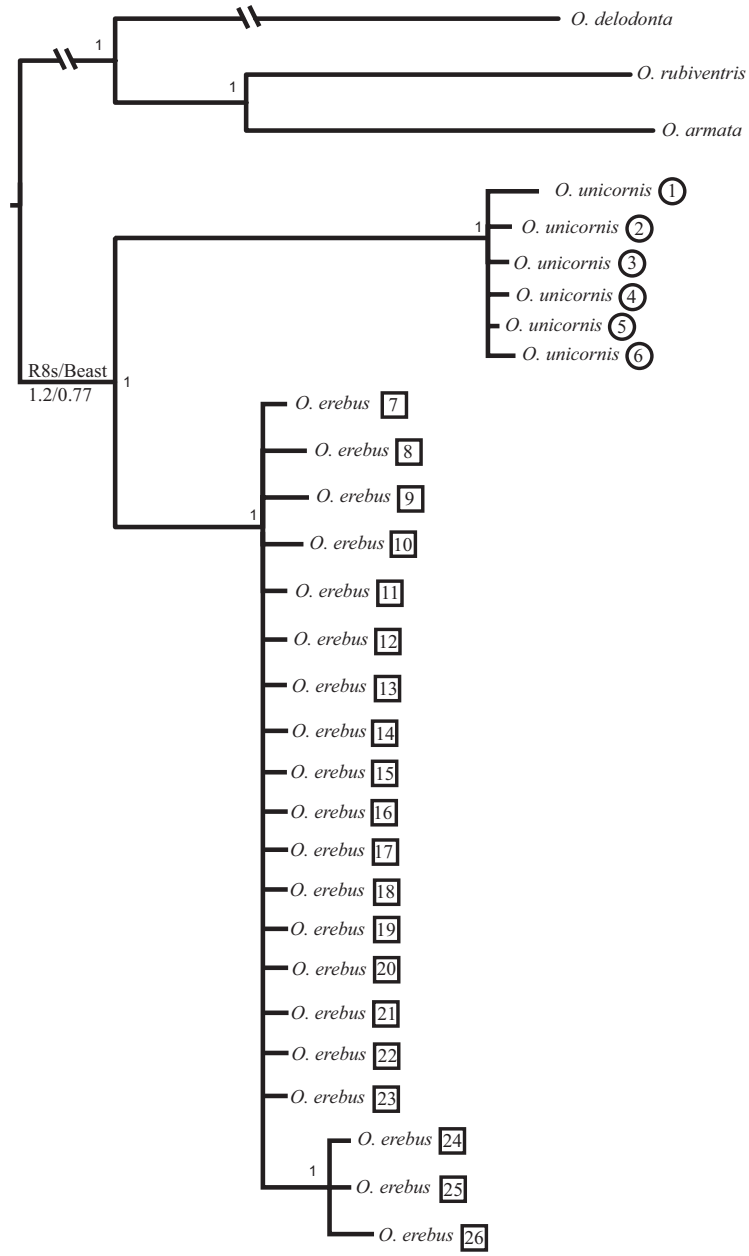

Fig. 2. Consensus tree of Bayesian analysis of the combined ITS1 and ITS2 sequences. Numbers at each node represent posterior probabilities. Symbols after species names correspond to symbols on the map of the distributions of the species in the *O. unicornis* species-group (see Fig. 1). The numbers within each symbol correspond to the Species ID no. in Table 1 which gives the exact collection location of each specimen. Estimated divergence dates are given for the node connecting *O. unicornis* and *O. erebus*.

third, the anterior margin of the clypeus is indistinctly emarginated, the ocellar area is concolorous with the head, and the cuspis is not narrowed medially having stout setae throughout (Figs. 9–12).

Diagnosis of Female. The female of *O. erebus* can be separated from the female of *O. unicornis* by the legs being concolorous with the body, and the decumbent setae on the dorsum of the mesosoma and second tergite of the metasoma being orangish brown to brown (Fig. 13).

Distribution. Widely distributed from western Kansas, Nebraska, Oklahoma, and Texas west to Arizona, Nevada, New Mexico, and Utah and south into northern Mexico. Absent from the Mojave, Great Basin, and western Sonoran deserts (Krombein 1979, Pitts 2007).

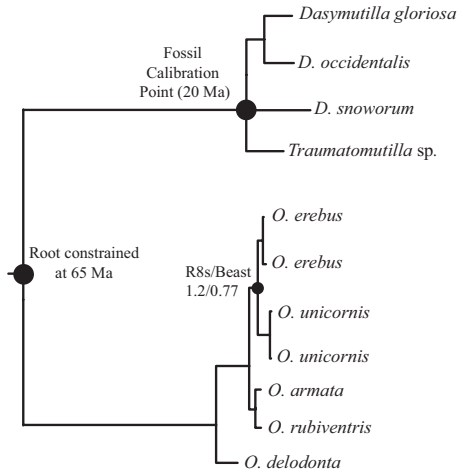

Fig. 3. Consensus tree of the Bayesian analysis done on the paired down data set. Black circles represent the calibration points that were used in the molecular dating analyses and the estimated divergence date for the *O. unicornis* species-group.

Remarks. The female of this species is fully described in Pitts et al. (2007), and the male of this species is discussed at length in Pitts (2007).

Odontophotopsis unicornis Schuster

Odontophotopsis (*Odontophotopsis*) *unicornis* Schuster, 1958. Entomol. Am. (n. s.) 37: 52. Male. Neotype: USA: AZ: Graham Co., 2.4 miles W Hwy 366 from Hwy 191, 3,800 feet, 14–26-VIII-1993, Hara (EMUS).

Diagnosis of Male. In this species, the clypeus is also concave with tuberculate process at median proximal margin, but the process is narrowly linguiform, is produced downward over clypeus, is prominent and is much longer than wide (Fig. 6). The anterior margin of the clypeus is distinctly emarginate and turned outward, the ocellar area usually is concolorous with the head, but sometimes slightly infuscated, the cuspis is slightly narrowed medially having an apex with stout setae, medially having thinner setae, and an inner margin with circular area of dense short setae (Figs. 9–12).

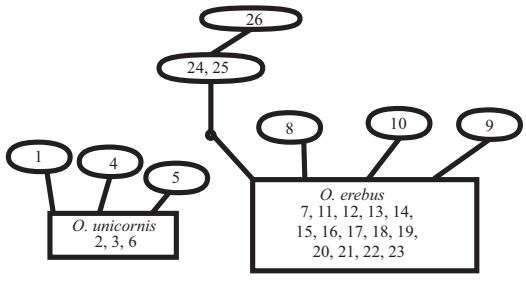

Fig. 4. Haplotype networks of *O. unicornis* and *O. erebus*. The number in each haplotype corresponds to the information in Table 1. Haplotypes surrounded by a rectangle were estimated to be the ancestral haplotype for each species.

Diagnosis of Female. The female of *O. unicornis* can be separated from the female of *O. erebus* by the legs being light yellow and not concolorous with the body, and the decumbent setae on the dorsum of the mesosoma and second tergite of the metasoma being bright orange (Fig. 14).

Description of Female. *Coloration and Setal Pattern.* Body reddish brown to brown; legs light yellow. Mandibular apex black. Flagellum light yellow to dark yellow. Decumbent setae dense, concealing sculpture of head and mesosomal dorsum; setae distinctly plumose especially at base of setal stalk. Head with dense decumbent white to pale golden plumose setae and erect white to pale golden brachyplumose setae. Genal region less densely pubescent. Anterior margin of pronotum, pleurae, and vertical face and lateral faces of propodeum with erect white brachyplumose setae. Dorsum of mesosoma with dense decumbent bright orange plumose setae and sparser erect brachyplumose setae; color changes to white laterally and on dorsal face of propodeum. T1 covered with erect white brachyplumose setae. T2 with decumbent orange plumose setae and erect brachyplumose setae. T1–T5 and S2–S5 with fringe of dense white fluffy plumose setae. Fringe of T2–T4 obscures proceeding disk. Legs with white brachyplumose setae.

Head. Head rounded posteriorly, not as wide as mesosoma, moderately punctate. Eye slightly ovate, distance from posterior mandibular articulation ≈2.5× visible length of pedicel. Clypeus protruding anteriorly, posteromedially produced into low triangular tubercle. Antennal scrobes lacking dorsal carina. Antennal tubercle with multiple carinae running parallel to apical margin. Flagellomere I ≈1.2× length of pedicel. Flagellomere II ≈1.2× and FIII ≈1.4× length of pedicel. Flagellomeres II–X produced apically on ventral side; appearing crenulate. Mandible bidentate apically. Ventral mandibular margin with basal angulation; excision as wide as 0.2× basal width of mandible. Genal carina absent.

Mesosoma. Mesosoma obpyriform, slightly longer than broad; broadest medially. Mesosoma densely confluently punctate on dorsum; punctures becoming larger posteriorly. Propleuron completely, mesopleuron medially running vertically, and extreme ventral region of propodeal side punctate. Humeral angle dentate. Epaulet prominent. Scutellar scale and transverse sinuate carina absent. Mesosternum with low transverse tubercle present medially just anterior to mesocoxa. Metasternum tridentate, median tooth ≈4× as long as lateral teeth. Mid and hind tibiae with two rows of spines on outer margin and each with pair of apical tibial spurs.

Metasoma. Segment one subpetiolate with segment 2. Tergite 1 with small sparse punctures. Tergite 2 with dense moderate punctures anteriorly; punctures becoming more widely spaced posteriorly (interstial distance ≥ puncture width). Tergite 2 with felt line; ≈0.33× length of tergite. Tergite 6 with distinct pygidial area defined laterally and apically by thickened

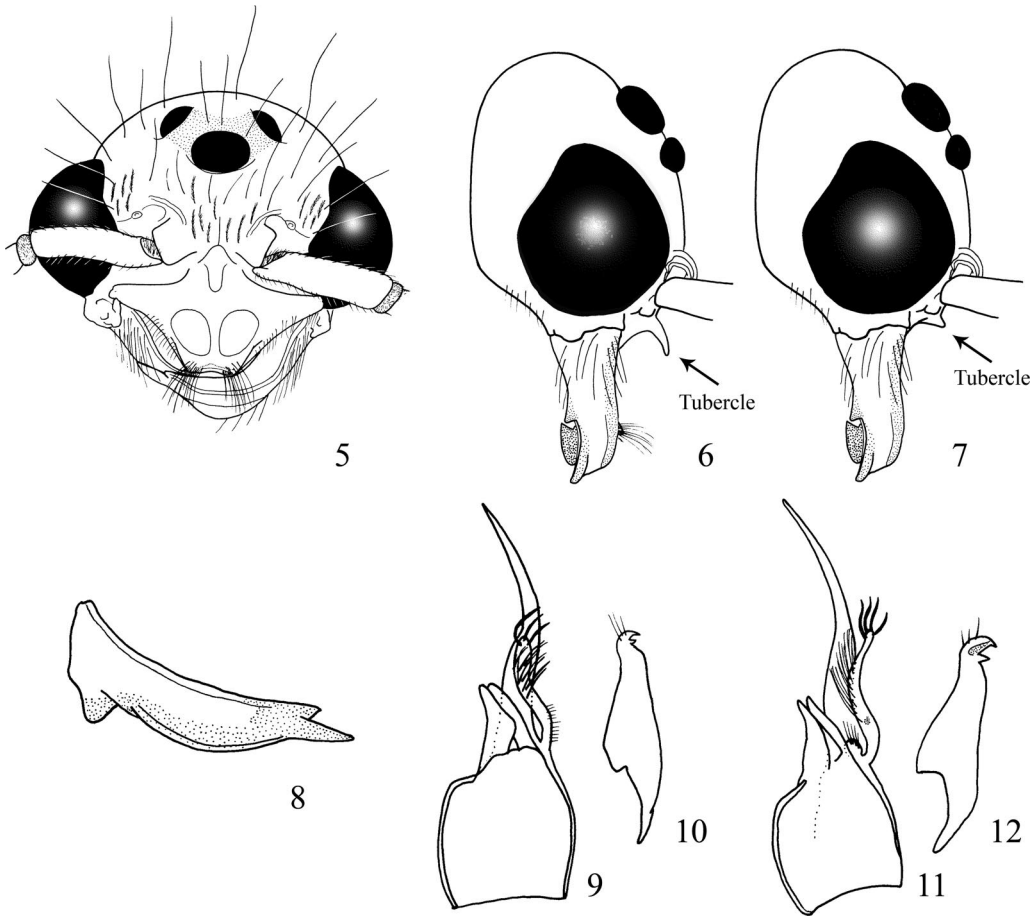

Figs. 5–12. *O. unicornis*: (5) Head, frontal view. (6) Head, lateral view. (8) Mandible. (9) Genitalia, lateral view. (10) Penal valve. *O. erebus*. (7) Head, lateral view. (11) Genitalia, lateral view. (12) Penal valve (see figs. 5, 6, 8–12 are from Pitts 2007; fig. 7 is from Pitts et al. 2010).

up-turned margin; surface weakly longitudinally striate throughout. Sternite 2 with slight anteromedian tumid region. Sternite 2–S5 with punctation similar to tergites.

Length. Length ≈6–9 mm.

Distribution. The Sonoran and Mojave Deserts of Arizona, Nevada, California into northern Mexico (Pitts 2007).

Fig. 13. Habitus of the female of *O. erebus*.

Fig. 14. Habitus of the female of *O. unicornis*.

Remarks. It is somewhat difficult to differentiate the species of the *O. unicornis* species-group based on females. This is not surprising given the difficulty of separating the females of other related taxa (Pitts et al. 2004, Pitts 2006). The two species basically differ only in setal and leg coloration, as well as that *O. unicornis* has slightly denser punctation on T2. The two species overlap greatly in range in southern Arizona, and in this area locality data are not a good indicator for identifying the females. The males of these species, however, are usually not difficult to distinguish and differ mainly in the shape and position of the tubercle on the clypeus (Figs. 1–3).

Discussion

Pitts (2007) stated that the distinction between the genitalia and clypeal tubercles of the males of the two species in the *O. unicornis* species-group can be occasionally difficult to discern, and future molecular data may show that these species represent one highly variable species. The present morphological and molecular analysis of the *O. unicornis* species-group, however, clearly indicates that the two species in this group are distinct (Fig. 2). Although the molecular distances between the species in this group are slightly lower than has been found in other mutillids (Wilson and Pitts 2008, 2009), the phylogenetic and haplotype analyses, together with the morphological characters, support the individuality of *O. unicornis* and *O. erebus.*

Several genetic analyses of mutillid wasps have shown that conspecifics often have identical or nearly identical ITS1 and ITS2 sequences (Pilgrim and Pitts 2006; Pitts et al. 2007, 2008). The genetic distances between the unknown females that were included in the analysis and *O. unicornis* were comparable with distances found in other sex-association studies and suggest that these females are *O. unicornis.*

The geographic distributions of these two species (Fig. 1) show similar patterns to other North American desert taxa, including other mutillid wasps, with one species being restricted to the eastern deserts (Chihuahuan and Great Basin deserts and the Colorado Plateau) and the other species restricted to the western deserts (Mojave and Sonoran deserts) (Morafka 1977, Riddle 1995, Wilson and Pitts 2008). An east–west split, like that seen in the *O. unicornis* species-group, has been observed in several other desert-adapted taxa and has often been associated with Neogene mountain building (Morafka 1977, Jaeger et al. 2005, Devitt 2006, Douglas et al. 2006). Morafka (1977) first attempted to explain the phenomenon of sister species being restricted to eastern and western deserts by describing a hypothetical ancient desert region called Mojavia, which extended from the modern Mojave Desert east through the Sonoran and Chihuahuan deserts. This vast desert region was subsequently split into eastern and western deserts by the uplift of the Continental Divide (made up of the Rocky Mountains and the Sierra Madre Mountains), which occurred in the late Neogene, from ≈15 to 2 Ma (Wilson and Pitts 2010). Although this scenario seems to explain the phylogeographic patterns in many animals, including other mutillid wasps (Jaeger et al. 2005, Devitt 2006, Douglas et al. 2006, Wilson and Pitts 2008), the estimated divergence date associated with the development of the *O. unicornis* species-group suggests that the evolution of these species was driven by more recent events.

Based on the proposed location of Pleistocene desert refugia, the pattern of sister species inhabiting eastern and western deserts could be attributed to effects of isolation in eastern and western refugia. Evidence of Pleistocene refugia for desert taxa exists in the Chihuahuan Desert (Elias et al. 1992) and the Sonoran Desert (Van Devender 1990, Van Devender et al. 1990, Hunter et al. 2001). If a species was widespread in the deserts during Pleistocene interglacials, it could have been forced into refugia in both the east and west during the onset of a glacial cycle. This isolation could have led to the same pattern of species distribution that has often been associated with Neogene mountain building. Divergence dates are necessary to be able to distinguish between Neogene and Pleistocene diversification.

Both divergence date estimations for the *O. unicornis* species-group suggest that the diversification within this group occurred during the mid to late Pleistocene (Fig. 2). Pleistocene age diversification has been found in population-level analyses (e.g., Ayoub and Riechert 2004); yet, the effect Pleistocene climate change had on species-level divergence has been questioned due to the lack of evidence (Klicka and Zink 1997). Divergence date calculations, such as these, can be affected by inadequate sampling; if taxa are considered to be sister species erroneously, the calculated divergence dates can be mistaken as younger than actual. Our results, however, of young divergence dates placed in the Pleistocene are not the artifact of an incorrect assumption of the monophyly of the *O. unicornis* species-group. *O. erebus* and *O. unicornis* are undoubtedly sister taxa. This conclusion is based on the degree of morphological similarity between these two species and also is based on a comparison of sequences of these two species with ≈75% of *Odontophotopsis* species and more complete phylogenetic analyses (e.g., Pitts et al. 2010; unpublished data). As such, this analysis, along with other recent studies (e.g., Pitts et al. 2010), provides strong evidence of species-level diversification being driven by Pleistocene climatic oscillations.

Unlike the phylogeographic patterns observed in other mutillid wasps (Wilson and Pitts 2008, 2009), there is little or no phylogenetic structure within either species in the *O. unicornis* species-group (Fig. 2). This lack of genetic structuring could be a result of extensive gene flow between distant populations, or it could be a result of relatively recent range expansion. Although the current study did not attempt to measure gene flow between populations, it is unlikely that the lack of variation in ITS1 and ITS2 among the populations of *O. unicornis* and *O. erebus* is due to wide-ranging gene flow. Population-level analyses of other mutillid wasps have shown genetic structuring

using both ITS1 and ITS2, so it is doubtful that the *O. unicornis* species-group species differ drastically in behavior that would cause extensive gene flow. The results of the molecular dating analyses suggest, however, that *O. unicornis* and *O. erebus* evolved recently in the mid to late Pleistocene and this recent origin could explain the lack of phylogenetic structure among distant populations. Because each species presumably did not evolve until the mid Pleistocene, there has not been sufficient time for remote populations to develop phylogenetically informative mutations in ITS1 or ITS2. Future fine-scale analyses, such as microsatellite analyses, may uncover population-level genetic structure among populations in the *O. unicornis* species-group.

Although Neogene geologic events have often been cited as the driving force behind the majority of species-level divergences in desert-adapted species, this study shows that not all taxa showing an east–west pattern of genetic divergence were influenced by the same historical events. Because both Neogene events and Pleistocene events can lead to similar patterns of genetic divergence, it is imperative that divergence dates are estimated so more accurate historical biogeographic hypotheses can be formed.

Acknowledgments

We thank Carol von Dohlen (Utah State University) for the use of laboratory space and equipment. We thank Erik Pilgrim and Carrie Drake for help with DNA extraction, PCR, and DNA sequencing. We thank Carol von Dohlen and Terry Griswold for reviewing previous drafts of this manuscript. Funding for this research was provided in part through the AMNH Theodore Roosevelt Memorial Fund grant and the Southwestern Research Station. Additional funding was provided through the California Desert Research Fund at The Community Foundation. This research also was supported by the Utah Agricultural Experiment Station, Utah State University, Logan, UT, and was approved as journal paper 8167.

References Cited

Avise, J. 2000. Phylogeography: the history and formation of species. Harvard University Press, Cambridge, MA.

Ayoub, N. A., and S. E. Riechert. 2004. Molecular evidence for Pleistocene glacial cycles driving diversification of a North American desert spider, *Agelenopsis aperta.* Mol. Ecol. 13: 3453–3465.

Bower, J. E., M. Dowton, R. D. Cooper, and N. W. Beebe. 2008. Intraspecific concerted evolution of the rDNA ITS1 in *Anopheles farauti* sensu stricto (Diptera: Culicidae) reveals recent patterns of populations structure. J. Mol. Evol. 67: 397–411.

Brothers, D. J. 1995. Mutillidae. pp. 541–548. *In* P. E. Hanson and I. D. Gauld (eds.), The Hymenoptera of Costa Rica. Oxford University Press, Oxford, NY.

Clement, M., D. Posada, and K. Crandall. 2000. TCS: a computer program to estimate gene genealogies. Mol. Ecol. 9: 1657–1660.

Devitt, T. J. 2006. Phylogeography of the western lyresnake (*Trimorphodon biscutatus*): testing aridland biogeographical hypotheses across the Nearctic-Neotropical transition. Mol. Ecol. 15: 4387–4407.

Douglas, M. E., M. R. Douglas, G. W. Schuett, and L. W. Porras. 2006. Evolution of rattlesnakes (Viperidae; *Crotalus*) in the warm deserts of western North America shaped by Neogene vicariance and Quaternary climate change. Mol. Ecol. 15: 3353–3374.

Drummond, A. J., and A. Rambaut. 2007. BEAST: Bayesian evolutionary analysis by sampling trees. BMC Evol. Biol. 7: 214.

Elias, S. A, J. I. Mead, and L. D. Agenbroad. 1992. Late quaternary arthropods from the Colorado plateau, Arizona and Utah. Great Basin Nat. 52: 59–67.

Ferguson, W. E. 1967. Male sphaeropthalmine mutillid wasps of the Nevada Test Site. Brigham Young Univ. Sci. Bull. Biol. Ser. 8: 1–26.

Grimaldi, D., and M. S. Engel. 2005. Evolution of the Insects. Cambridge University Press, New York.

Harris, D. J., and K. A. Crandall. 2000. Intragenomic variation within ITS1 and ITS2 in freshwater crayfishes (Decapoda: Cambaridae): implications for phylogenetics and microsatellite studies. Mol. Biol. Evol. 17: 284–291.

Hunter, K. L., J. L. Betancourt, B. R. Riddle, T. R. Van Devender, K. L. Cole, and W. G. Spaulding. 2001. Ploidy race distributions since the Last Glacial Maximum in the North American desert shrub, *Larrea tridentata.* Global Ecol. Biogeogr. 10: 521–533.

Iturralde-Vinent, M. A., and R.D.E. MacPhee. 1996. Age and Paleogeographical origin of Dominican amber. Science 273: 1850–1852.

Jaeger, J. R., B. R. Riddle, and D. F. Bradford. 2005. Cryptic Neogene vicariance and Quaternary dispersal of the red-spotted toad (*Bufo punctatus*): insights on the evolution of North American warm desert biotas. Mol. Ecol. 14: 3033–3048.

Klicka, J., and R. M. Zink. 1997. The importance of recent ice ages in speciation: a failed paradigm. Science 277: 1666–1669.

Krombein, K. V. 1979. Mutillidae, pp. 1276–1314. *In* K. V. Krombein, P. D. Hurd, Jr., D. R. Smith, and B. D. Burks (eds.), Catalog of Hymenoptera in America North of Mexico. Smithsonian Institution Press, Washington, DC.

Lanave, C., G. Preparata, C. Saccone, and G. Serio. 1984. A new method for calculating evolutionary substitution rates. J. Mol. Evol. 20: 86–93.

Leaché, A. D., and D. G. Mulcahy. 2007. Phylogeny, divergence times and species limits of spiny lizards (*Sceloporus magister* species group) in western North American deserts and Baja California. Mol. Ecol. 16: 5216–5233.

Manley, D. G., and G. O. Poinar, Jr. 1991. A new species of fossil *Dasymutilla* (Hymenoptera: Mutillidae) from Dominican amber. Pan-Pac. Entomol. 67: 200–205.

Manley, D. G., and G. O. Poinar, Jr. 1999. A second species of fossil *Dasymutilla* (Hymenoptera: Mutillidae) from Dominican amber. Pan-Pac. Entomol. 75: 48–51.

Manley, D. G., and G. O. Poinar, Jr. 2003. A new specimen of fossil Mutillidae (Hymenoptera) from Dominican amber. Proc. Entomol. Soc. Wash. 105: 1069–1071.

Melander, A. L. 1903. Notes on North American Mutillidae, with descriptions of new species. Trans. Am. Entomol. Soc. 29: 219–330.

Morafka, D. J. 1977. A biogeographical analysis of the Chihuahuan Desert through its herpetofauna. Dr. W. Junk, The Hauge, The Netherlands.

Nonveiller, G. 1990. Hymenopterorum catalogus: (nova editio). Pars 18: Catalogue of the Mutillidae, Myrmosidae and Bradynobaenidae of the Neotropical Region including Mexico (Insecta: Hymenoptera). SPB Academic Publishing, The Hague, The Netherlands.

Nylander, J.A.A. 2004. MrModeltest, version 2. Evolutionary Biology Centre, Uppsala University. Uppsala, Sweden.

Orange, D. I., B. R. Riddle, and D. C. Nickle. 1999. Phylogeography of a wide-ranging desert lizard, *Gambelia wislizenii* (Crotaphytidae). Copeia 1999: 267–273.

Parkin, E. J., and R. K. Butlin. 2004. Within- and between-individual sequence variation among ITS1 copies in the meadow grasshopper *Chorthippus parallelus* indicates frequent intrachromosomal gene conversion. Mol. Biol. Evol. 21: 1595–1601.

Pilgrim, E. M., S. A. Roush, and D. E. Krane. 2002. Combining DNA sequences and morphology in systematics: testing the validity of the dragonfly species *Cordulegaster bilineata.* Heredity 89: 184–190.

Pilgrim, E. M., and J. P. Pitts. 2006. A molecular method for associating the dimorphic sexes of velvet ants (Hymenoptera: Mutillidae). J. Kans. Entomol. Soc. 79: 222–230.

Pilgrim, E. M., K. A. Williams, and J. P. Pitts. 2008. Sex association and synonymy in southwestern U.S. species of *Dasymutilla* (Hymenoptera: Mutillidae). Pan-Pac. Entomol. 84: 58–69.

Pitts, J. P. 2006. Review of the *Sphaeropthalma imperialis* species-group (Hymenoptera: Mutillidae), with descriptions of females and taxonomic notes. Zootaxa 1248: 1–20.

Pitts, J. P. 2007. Revision of *Odontophotopsis* Viereck (Hymenoptera: Mutillidae), Part 1, with a description of a new genus *Laminatilla.* Zootaxa 1619: 1–43.

Pitts, J. P., F. D. Parker, and T. L. Pitts-Singer. 2004. A review of the *Sphaeropthalma uro* species-group (Hymenoptera: Mutillidae), with taxonomic changes. J. Kans. Entomol. Soc. 77: 223–234.

Pitts, J. P., T. J. Boud, and E. M. Pilgrim. 2007. Molecular sex association of three species of nocturnal velvet ant (Hymenoptera: Mutillidae). J. Kans. Entomol. Soc. 80: 136–145.

Pitts, J. P., J. S. Wilson, K. A. Williams, and N. Boehme. 2009. The velvet ants (Hymenoptera: Mutillidae) of the Algodones sand dunes of California, USA. Zootaxa 2131: 1–53.

Pitts, J. P., J. S. Wilson, and C. D. von Dohlen. 2010. Evolution of the nocturnal Nearctic Sphaeropthalminae velvet ants (Hymenoptera: Mutillidae) driven by Neogene Orogeny and Pleistocene glaciation. Mol. Phylogenet. Evol. 56: 134–145.

Riddle, B. R. 1995. Molecular biogeography in the pocket mice (*Perognathus* and *Chaetodipus*) and grasshopper mice (*Onychomys*): the late Cenozoic development of a North American aridlands rodent guild. J. Mammal. 76: 283–301.

Ronquist, F., and J. P. Huelsenbeck. 2003. Mrbayes 3: Bayesian phylogenetic inference under mixed models. Bioinformatics 19: 1572–1574.

Sanderson, M. J. 2003. R8s: inferring absolute rates of molecular evolution and divergence times in the absence of a molecular clock. Bioinformatics 19: 301–302.

Schuster, R. M. 1958. A revision of the sphaeropthalmine Mutillidae of America north of Mexico. II. Entomol. Am. 37: 1–130.

Thompson, J. D., D. G. Higgins, and T. J. Gibson. 1994. CLUSTAL W: improving the sensitivity of progressive multiple sequence alignment through sequence weighting, position-specific gap penalties and weight matrix choice. Nucleic Acids Res. 22: 4673–4680.

Van Devender, T. R. 1990. Late Quaternary vegetation and climate of the Chihuahuan Desert, United States and Mexico. pp. 104–133. *In* J. L. Betancourt, T. R. Van Devender, and P. S. Martin (eds.), Packrat middens: the last 40,000 years of biotic change. University of Arizona Press, Tucson. AZ.

Van Devender, T. R., T. L. Burgess, R. S. Felger, and R. M. Turner. 1990. Holocene vegetation of the Harnaday Mountains of Northwestern Sonora, Mexico. Proc. San Diego Soc. Nat. Hist. 2: 1–19.

Viereck, H. L. 1904. The species of *Odontophotopsis.* Am. Entomol. Soc. Trans. 30: 81–92.

Weekers, P.H.H., J. F. De Jonckheere, and H. J. Dumont. 2001. Phylogenetic relationships inferred from ribosomal ITS sequences and biogeographic patterns in representatives of the genus *Calopteryx* (Insecta: Odonata) of the West Mediterranean and adjacent West European zone. Mol. Phylogenet. Evol. 20: 89–99.

Wilson, J. S., and J. P. Pitts. 2008. Revision of velvet ant genus *Dilophotopsis* Schuster (Hymenoptera: Mutillidae) by using molecular and morphological data, with implications for desert biogeography. Ann. Entomol. Soc. Am. 101: 514–524.

Wilson, J. S., and J. P. Pitts. 2009. Species boundaries of *Sphaeropthalma unicolor* (Hymenoptera: Mutillidae): is color useful for differentiating species? J. Hymenopt. Res. 18: 212–226.

Wilson, J. S., and J. P. Pitts. 2010. Illuminating the lack of consensus among descriptions of earth history data in the North America deserts: a resource for biologists. Prog. Phys. Geo. (DOI: 10.1177/0309133310363991).

Received 11 December 2009; accepted 5 April 2010.